Demand-Side Management Using Deep Learning for Smart Charging of Electric Vehicles

Article *in* IEEE Transactions on Smart Grid · February 2018

DOI: 10.1109/TSG.2018.2808247

3 authors, including:

Karol Lina Lopez
RAMQ
10 PUBLICATIONS **280** CITATIONS

SEE PROFILE

Christian Gagné
Université Laval
175 PUBLICATIONS **5,192** CITATIONS

SEE PROFILE

Demand-Side Management using Deep Learning for Smart Charging of Electric Vehicles*

Karol Lina López, Christian Gagné, and Marc-André Gardner
Computer Vision and Systems Laboratory, Université Laval, Québec, QC, G1V 0A6 Canada
karol-lina.lopez.1@ulaval.ca, christian.gagne@gel.ulaval.ca, marc-andre.gardner.1@ulaval.ca

February 17, 2018

Abstract

The use of Electric Vehicles (EVs) load management is relevant to support electricity demand softening, making the grid more economic, efficient, and reliable. However, the absence of flexible strategies reflecting the self-interests of EV users may reduce their participation in this kind of initiative. In this work, we are proposing an intelligent charging strategy using Machine Learning (ML) tools, to determine when to charge the EV during connection sessions. This is achieved by making real-time charging decisions based on various auxiliary data, including driving, environment, pricing, and demand time series, in order to minimize the overall vehicle energy cost. The first step of the approach is to calculate the optimal solution of historical connection sessions using dynamic programming. Then, from these optimal decisions and other historical data, we train ML models to learn how to make the right decisions in real time, without knowledge of future energy prices and car usage. We demonstrated that a properly trained deep neural network is able to reduce charging costs significantly, often close to the optimal charging costs computed in a retrospective fashion.

Abbreviations

AC Always Charge
DNN Deep Neural Network
DP Dynamic Programming
DSM Demand-Side Management
EV Electric Vehicle
HOD Hourly Ontario Demand
HOEP Hourly Ontario Energy Price
KNN k-Nearest Neighbors
MDP Markov Decision Process
ML Machine Learning
PHEV Plug-in Hybrid EV
SNN Shallow Neural Network
SoC State of Charge
TBR Threshold-Based Rule

1 Introduction

In the context of a smart grid, Demand-Side Management (DSM) aims at proposing incentive-based measures to influence electricity consumption patterns, such that a more efficient use of energy is made. This often ensures that the existing infrastructure is efficiently used, in order to meet increased demand and to minimize investments in additional generation capacity [1]. Given the widespread adoption of Electric Vehicles (EVs), which could increase the risk of overloading the power grid by inflating demand peaks, there is a particular interest for integrating DSM

*Cite this paper as: "Karol Lina López, Christian Gagné, and Marc-André Gardner, Demand-Side Management using Deep Learning for Smart Charging of Electric Vehicles, *IEEE Transactions on Smart Grid* (in-press), 2018."

into EV charging using economic incentives such as dynamic prices. However, most recent studies have revealed the lack of knowledge among EV users on how to respond to time-varying prices, which may considerably reduce their participation in DSM programs [2, 3, 4, 5]. These studies have focused more on smart charging of EVs considering centralized and decentralized perspectives [6].

A classical decision-making approach for the smart charging problem would include two components: 1) predicting the future states of environmental and behavioral variables (e.g., electricity cost, driving habits) and 2) making optimal decisions given these predictions. But the optimality of these decisions is possible only with perfect knowledge of the future. In practice, the decision-making aspect is likely to encounter difficulty when there are significant variations on predicted values, by not being able to take into account the prediction uncertainty, for example when different outcomes are likely.

Instead of devising a better prediction system, we propose an end-to-end learning approach where predictions and actions are jointly optimized. This Machine Learning (ML)-based approach allows real-time decisions in any context, providing some flexibility to every EV user in order to satisfy their own needs and goals. Moreover, it removes the need for hand-crafted, analytic decision functions, which can be tedious to express in the general case. Our method automatically learns this decision function, implicitly taking into account the strengths and weaknesses of the prediction function. It also allows personalized decision functions to be learned, by training the model with user-specific data.

In particular, we are proposing in this paper a demand response strategy based on ML to control the EV charging in response to the real-time pricing, such that the overall energy cost of an EV is minimized. First, we use the Markov Decision Process (MDP) framework to model a discrete time interval charging control process, where, at each time interval, a decision is made on the action to take in order to reach the goal. We address this problem using Dynamic Programming (DP), assuming that we have complete information on the current and future states, such as prices (electricity and gasoline) and trips (distance and time). Then, the optimal actions found with DP become the desired targets to learn, in order to infer from historical data a function that can properly map complex inputs representing the current state to charging decisions. Finally, a comparison on the cost (in $CAD) is made between several ML algorithms: Deep Neural Network (DNN), Shallow Neural Network (SNN), and k-Nearest Neighbors (KNN). We also provide results for two additional baseline models: Always Charge (AC) when possible and Threshold-Based Rule (TBR), in which we make the decision based on a thresholding on the electricity price. We compare these methods to the optimal offline solution obtained with DP. Results show that DNN significantly outperforms the other models proposed for real-time decision-making, approaching the optimal decision obtained with DP, while not requiring knowledge of the future.

The paper is organized as follows. Sec. 2 presents the related work. In Sec. 3, we show the general methodology proposed for smart charging of EVs in a perspective of making decisions in real time. Experiments, results and analysis with the proposed ML approaches, such as DNN are presented in Sec. 4, before concluding on the relevant findings in Sec. 5.

2 Related Work

Integration of EVs and DSM can be organized with a centralized and a decentralized coordination perspective [7]. Moreover, the primary objective is varied: frequency or voltage regulation [8], minimization of the generation cost [9], reduction of charging cost [10, 11], reduction of power losses [12], maximization of the load factor or minimization of the load variance [13], and valley-filling in electric load profiles [14]. In the centralized perspective, a single agent (smart grid or aggregator) directly manages the charging of all EVs, which requires prior knowledge of a large amount of data to reach an optimal solution [15]. On the contrary, a decentralized perspective assumes that the EV's owners have complete control over their charging decisions, giving them more flexibility to participate in DSM programs and so to respond to different price signals [16]. Several dynamic prices have been proposed as an incentive for volunteer participation of the EV users in DSM programs, although only flat rates such as Time-of-Use

pricing (ToU pricing) have been adopted [17]. Compared to the current flat rates, real-time pricing is considered the best cost-effective solution for both utilities and EV users to prevent EV-charging peak in off-time periods [18]. Considerable efforts have been made to optimally schedule the charging of EVs in order to minimize the usage cost of EVs [11, 19, 20]. However, an optimized schedule can only be achieved with precise information about the future, and such a schedule is thus difficult to make and can be impractical, unscalable and risky with respect to speculation, leading to inefficient schedules that are not based on actual EV user requirements.

In the meantime, significant hardware and algorithmic developments involving ML have shown astonishing results for complex problems in many fields. In particular, DNN is a disruptive approach in areas as diverse as computer vision and natural language processing [21]. With reference to time-series analysis, recent efforts are increasingly focused on the deep learning approach [22]. **(author?)** [23] use a DNN for short-term load forecasting while **(author?)** [24] proposed the use of DNN for the prediction of energy consumption. DNN for time-series classification problems is also documented by **(author?)** [25]. In this regard, we are focussing on the convergence between the recent ML algorithms and the strategies proposed so far to produce a methodology that can be applied to the smart charging of EVs or in many other similar decision-making problems, e.g., DSM for smart appliances.

3 Proposed Methodology

Fig. 1 presents the global methodology proposed to train a decision-making model for smart charging of EVs responding in real time to a dynamic electricity pricing. The *datasets* stage shows the different sources used for the experiments, as well as additional related information (Sec. 3.1). The *optimization* stage uses DP on MDP modelling to compute the optimal solutions (Sec. 3.2). The historical datasets and the corresponding optimal solutions are then joined in an *information system* to produce the training and testing sets (Sec. 3.3). Finally, ML algorithms are used for the *learning* of models from the datasets (Sec. 3.4).

3.1 Datasets

The GPS-based usage data was collected from 17 different conventional cars in the city of Winnipeg, Manitoba, Canada. This database[1] includes trip number, date, time, position, actual speed, and maximum allowable speed at the vehicle's location, with a time granularity of one second [26]. An overview of the distances travelled in summer and winter as well as the maximum distance found is presented in Table 1.

From these data we simulate trips and charging sessions of Plug-in Hybrid EV (PHEV). To enable a comparison, we used the same specification for all vehicles, especially regarding the battery (Table 5). This specification corresponds to a PHEV similar to the Chevrolet Volt and some parameters of Panasonic Lithium-ion NRC18650 batteries, as the full specifications of the Volt batteries are not publicly available.

The energy dataset is composed of the Hourly Ontario Energy Price (HOEP) and the Hourly Ontario Demand (HOD)[2]. HOEP is the hourly price that is charged to local distribution companies in Ontario, Canada. Although it does not correspond exactly to the price domestic consumers are paying for energy in Ontario, it provides a good indicator of the electricity price on an hourly frequency. HOD represents the sum of all loads supplied from the market on an hourly base, plus all line losses incurred on the IESO-controlled grid.

The historical data of outdoor air temperature recorded at the Waterloo Weather Station[3] was also included, since electricity price and demand are, among other factors, correlated to temperature. Finally, we used the weekly average consumers price of regular unleaded gasoline provided by the Ontario Ministry of Energy. This database[4] is useful to evaluate the cost of driving on the combustion engine.

[1] `http://hdl.handle.net/1993/8131`
[2] `http://www.ieso.ca/power-data`
[3] `http://weather.uwaterloo.ca/data.html`
[4] `http://www.energy.gov.on.ca/en/fuel-prices`

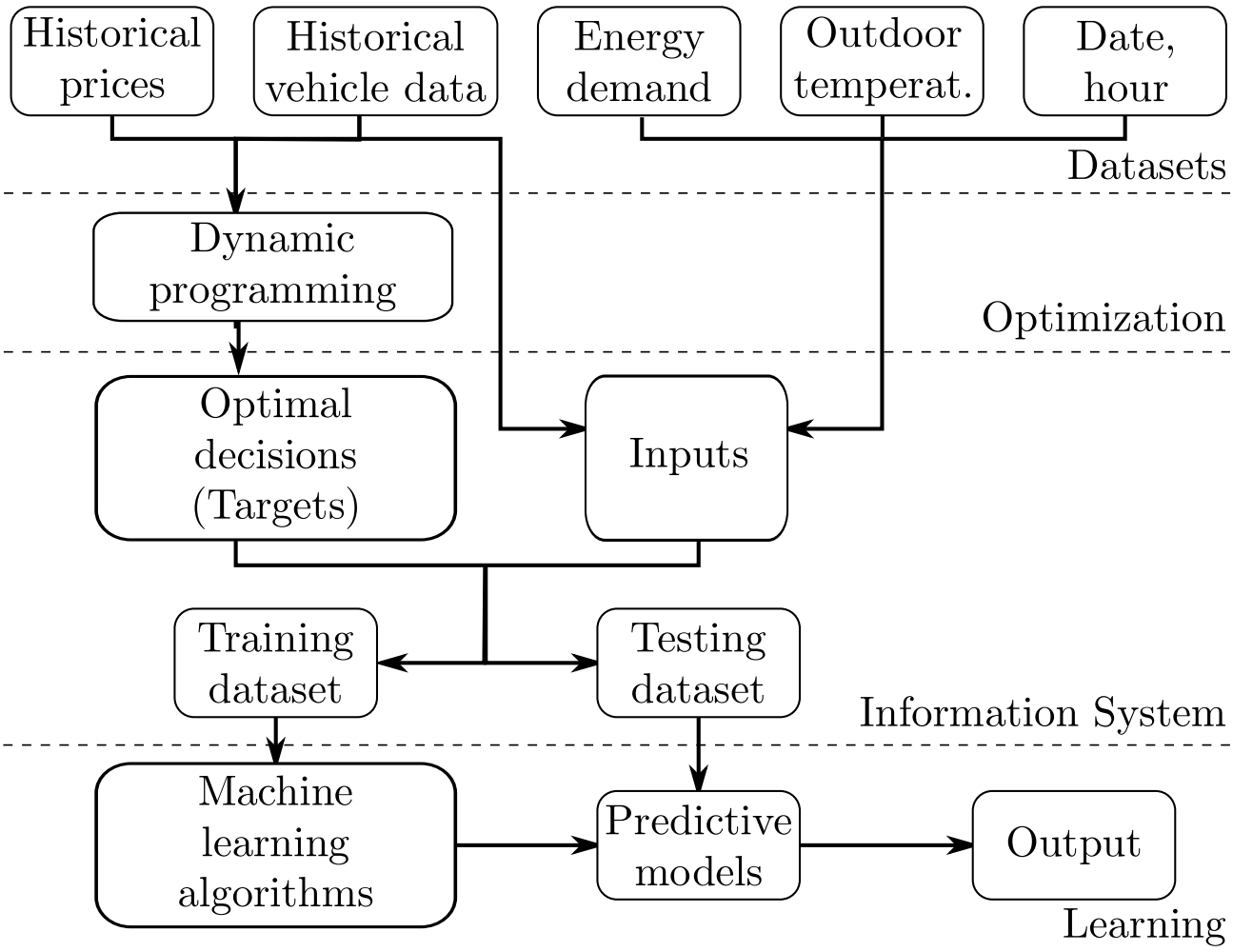

Figure 1: Overview of proposed methodology.

Table 1: Total and single trip maximum distance by vehicles in the test periods (in km).

	Summer		**Winter**	
	Total dist.	**Max. trip dist.**	**Total dist.**	**Max. trip dist.**
1	1637.37	28.23	1237.71	14.19
2	1168.62	27.76	859.85	25.50
3	656.68	19.97	664.82	23.93
4	2350.64	26.97	1270.42	25.47
5	2900.32	28.24	1116.17	17.11
6	1167.76	20.57	1507.47	24.56
7	1014.58	14.36	764.44	14.61
8	831.60	25.08	819.72	21.59
9	2866.43	27.64	611.79	25.09
10	806.70	12.37	1269.14	22.08
11	1961.95	25.31	2063.67	19.50
12	906.66	18.43	1215.06	15.27
13	4566.47	27.04	3392.94	27.52
14	1531.83	13.21	687.71	11.04
15	261.38	9.00	1176.91	12.30
16	400.00	19.09	1006.86	12.96
17	726.37	23.01	451.03	12.13

Table 2: Specifications of battery packs, based on Chevrolet Volt 2013 and Panasonic NRC18650 Li-Ion batteries.

Chevrolet Volt 2013 specifications	
Nominal System Voltage V_{nom}	355.2 V
Rated Pack Capacity Q_{nom}	45 Ah
Rated Pack Energy E_v	16.5 kWh
Fuel economy (electricity) m_e	98 mpg_e (35 kWh/100 miles)
Fuel economy (gasoline) m	37 mpg
Panasonic NRC18650 specifications	
Nominal Capacity Q_{nom}	2.75 Ah
Nominal Cell Voltage V_{cell}	3.6 V
Max. Cell Charge Voltage V_{max}	4.2 V
Cut-off Discharge Voltage V_{min}	2.5 V
Maximum Charge Current I_{max}	0.825 A
Constant Current Discharge I_{dh}	0.55 A
Cut-off Charge Current I_{min}	0.05 A

3.2 Optimization

The goal of the optimization of the smart charging of EVs is to obtain the optimal charging scheduling of an EV, determining the sequence of actions to take at each time interval of fixed duration (e.g., 15-minute periods), while the EV is plugged in, in order to minimize overall energy costs required to satisfy the EV's owner's needs.

We propose to use the MDP framework to model the transitions from one State of Charge (SoC) to another according to the actions taken. The mathematical equation of the cost objective function for determining the optimal actions is divided into two parts corresponding to two states, namely when the car is plugged in to a charging station (S_p) and when it is not (S_u). When the vehicle is plugged in, the cost function depends on the electricity price and the decision to charge or not, and can be described as:

$$S_p(t) = a(t) \cdot C_{el}(t) \frac{E_{ch}(SoC(t))}{\eta}, \tag{1}$$

where:

- $a(t)$ is the decision variable on whether the vehicle is being charged (1) or on standby (0) at time t;
- $C_{el}(t)$ is the electricity price [$/kWh] at time t;
- $E_{ch}(SoC(t))$ is the energy [kWh] supplied to the battery when charging is conducted during a fixed time interval, with battery state of charge $SoC(t)$ at the beginning of the period — charging rate (in kW) varies considerably depending on the current battery charge level;
- $\eta \in [0, 1]$ is the charger efficiency;
- $SoC(t)$ is the state of charge (fraction of the nominal battery capacity) at time t.

Due to space limitations, the model used to evaluate SoC and to compute the energy supplied to the battery is given in the Appendix.

When the vehicle is not plugged in, the cost is null except when the battery is depleted, in which case the vehicle must fall back to the gas engine. In this case, the following equation applies:

$$S_u(t) = C_{fuel}(t) \cdot k_{ge} \cdot \max(E_{dis} - E_{nom} \cdot SoC(t), 0), \tag{2}$$

where:

- $C_{fuel}(t)$ is the gasoline price [$/l] at time t;
- k_{ge} is a constant [l/kWh] allowing energy to be converted into volume of gasoline;
- E_{dis} is the amount of energy [kWh] consumed by the vehicle at time t;
- E_{nom} is the nominal capacity [kWh] of the battery.

Combining Eq.1 and Eq.2 yields the global optimization objective:

$$\min_{\{a(t)\}_{t=1}^{T}} \sum_{t=1}^{T} \left[z(t) \cdot S_p(t) + (1 - z(t)) \cdot S_u(t) \right], \tag{3}$$

where $z(t)$ returns a Boolean value indicating whether the vehicle is plugged in (1) or not (0) to a charging station at the time interval t.

In the case of PHEV, the energy consumed E_{dis} may be greater than the energy available in the all-electric range, given that the gas engine functions as a backup when the batteries are depleted. In the case of a battery

electric vehicle (BEV), $C_{fuel}(t)$ can be modified for an arbitrary stronger penalty associated with running out of energy.

Several measures may be considered to resolve the problem formulated in Eq. 3. We propose to formulate this problem into a recursive form that can be solved through DP [27]. Let us define the $Q(s(t), a)$ function as holding values in a three-dimensional array, with values evaluated recursively backwards (i.e., $t = T, T-1, \ldots, 1$), over all the states $s \in \mathcal{S}$ and actions $a \in \mathcal{A}$. This formulation requires the discretization of the SoC of the battery, which represents the current battery capacity as a percentage of maximum capacity (0% = empty; 100% = full) and the actions are *charging* or *standby*. $Q(s(t), a)$ is computed as:

$$Q(s(t), a) = \begin{cases} s(t) \cdot \overline{C_{el}} & \text{if } t = T \\ r(s(t), a) + & \\ \quad \max\limits_{a \in \mathcal{A}} Q(s(t+1), a) & \text{otherwise} \end{cases}, \tag{4}$$

where:

- $\overline{C_{el}}$ is the average electricity price over $t = 1, \ldots, T$;
- $s \in \mathcal{S}$ is a discretized value of the SoC over B bins:

$$s(t) = \frac{\lfloor SoC(t) \cdot B \rfloor + 0.5}{B}, \tag{5}$$

  where B is the number of bins used to discretize the charge levels[5];
- $a \in \mathcal{A}$ are the actions, with $\mathcal{A} = \{0, 1\}$, $a = 1$ corresponding to charging and $a = 0$ to standby mode;
- $r(s(t), a)$ is the immediate cost function (reward):

$$r(s(t), a) = \begin{cases} 0 & \text{if } z(t) = 1 \text{ and } a = 0 \\ -C_{el}(t) \frac{E_{ch}(SoC(t))}{\eta} & \text{if } z(t) = 1 \text{ and } a = 1 \\ g(SoC(t)) & \text{if } z(t) = 0 \end{cases}. \tag{6}$$

For the case when the EV is connected ($z(t) = 1$) and charging ($a(t) = 1$), $C_{el}(t) \cdot E_{ch}(SoC(t))/\eta$ provides the cost of energy actually transferred to the battery. $z(t) = 0$ corresponds to the case when the vehicle is on a trip and $g(SoC(t)) > 0$ appears when the energy consumed is greater than what is available in batteries, such that the gas engine is used.

The resolution by DP is deemed to be exact by following Bellman's *Principle of Optimality* [27]. Indeed, in Eq. 4, the charging problem is decomposed into small independent subproblems organized according to time and SoC. The exact resolution of this problem has a polynomial time and space complexity, that is $O(TB)$.

Once the values of the 3D array composing the $Q(s(t), a)$ function are computed by DP, the decisions are computed as:

$$a^*(t) = \underset{a \in \mathcal{A}}{\operatorname{argmax}}\ Q(s(t), a). \tag{7}$$

This allows the selection of the action according to the best corresponding Q-value. Up to the discretization of the SoC, this resolution by DP provides optimal solutions to the optimization problem presented as Eq. 3. The computational complexity, and therefore the speed of the DP model, is a direct function of the number of states (bins) in which the variable SoC is discretized and the number of time steps T.

[5]The effect of this approximation can be mitigated by a high B parameter value.

3.3 Information System

Traditionally, the information used in optimization methods has been modelled using probabilistic methods, incorporating random or forecasted variables in a model which leaves too much room for uncertainty. To address this issue, we are proposing to build an information system in order to explore real and diverse data to derive patterns using ML algorithms to make effective real-time decisions.

The creation of information systems consists in handling the multiple-time series variables, e.g., electricity prices and demand in arrays on discrete-time intervals with scalar data, consisting of data where only one decision is generated at each time, e.g., hourly or daily. Let $s = s(t) \in \mathcal{S}$, $t = 1, 2, ..., T$, where T is the number of data points used for the estimation. Each data point is the state of the system at time t, which can be represented as a vector composed of several delays embedding time series and other scalar variables. The process of building the space state is known as phase space reconstruction [28].

More formally, let $M = \{X^i\}_{i=1}^m$ be the m time series at hand, where each time series $X^i = \{x^i(t)\}_{t=1}^T$ is described by T data points. Let $\boldsymbol{u}^i = [u_1^i, u_2^i, \ldots, u_{n^i}^i] \in \mathbb{N}^{1\times n^i}$ be the n^i lags of a time series $\boldsymbol{v}^i \in \mathbb{R}^{1\times n^i}$ over variable $x^i(t)$ (e.g., energy price), and p be scalar variables assembled in vector $\boldsymbol{w} \in \mathbb{R}^{1\times p}$ (e.g., time of day). Thus, a state $\boldsymbol{s}(t) \in \mathbb{R}^{1\times d}$, with $d = p + \sum_{i=1}^m n^i$, can be built as follows:

$$\boldsymbol{u}^i = [u_1^i, \ldots, u_{n_i}^i],\ i = 1, \ldots, m, \tag{8}$$

$$\boldsymbol{v}^i(t) = [x^i(t - u_1^i), \ldots, x^i(t - u_{n^i}^i)],\ i = 1, \ldots, m, \tag{9}$$

$$\boldsymbol{w}(t) = [w_1, \ldots, w_p], \tag{10}$$

$$\boldsymbol{s}(t) = [\boldsymbol{v}^1(t)\| \cdots \|\boldsymbol{v}^m(t)\|\boldsymbol{w}(t)], \tag{11}$$

where $\|$ denotes the concatenation operator.

In this work we are comparing the data of two periods of time: summer 2008 and winter 2009. More specifically, we are using data from the months of June and July 2008 as the training set in summer and August 2008 as the testing set. Similarly, for winter 2009 we are using December 2008 and January 2009 as the training set and testing on February 2009.

The following variables have been selected:

- HOEP ($\boldsymbol{x}^1$), HOD ($\boldsymbol{x}^2$), and air temperature ($\boldsymbol{x}^3$) with lags ($\boldsymbol{v}^1 \in \mathbb{R}^{1\times n^1}$) where $n^1 = 101$: one-hour values for the last 72 hours (72 values), one-hour values at the same time for the days 3,4,5,6,7 before the current time (5 values), and one-hour values for the same day of the last week (24 values);
- Energy consumed ($\boldsymbol{x}^4$) with lags ($\boldsymbol{v}^2 \in \mathbb{R}^{1\times n^2}$), where $n^2 = 199$: energy consumed in 15-minute intervals for the last day (96 values), total energy consumed daily in the 7 days before (7 values), energy consumed in 15-minute intervals for the same day of the previous week (96 values);
- Scalar variables (converted into real values when necessary and normalized in the range $[0, 1]$):
  - w_1 : weekdays;
  - w_2 : hour;
  - w_3 : $C_{el}(t-1) - C_{el}(t)$ is the difference in electricity price [$/kWh] between $t-2$ and $t-1$;
  - w_4 : $C_{el}(t)$ is the electricity price [$/kWh] at time t;
  - w_5 : $C_{fuel}(t)$ is the gasoline price [$/l] at time t;
  - w_6 : $dis(t)$ is the distance travelled [km] at time t.

The number of instances in the training set N corresponds to the multiplication between the number of time steps T, the number of actions A, the number of vehicles V and the number of bins B (one bin being a different state of

charge), $N = T \times A \times V \times B$, with a dimensionality equivalent to $d = \sum_{i=1}^{m} n^i + p = 508$. We used the scheme proposed in [29] to treat the anomalous electricity prices and to standardize the data set on the feature component when the variables have different units.

3.4 Learning

DP actually allows optimal decisions to be made up to some approximations (related to variable discretizations) on historical databases, given that all the car and environmental data, including future values, are known in advance. We are proposing to use DP to label historical databases using the state space representation presented in the previous section. With these labelled data, we can use standard supervised learning algorithms to infer models that can handle real-time decisions related to the task at hand (i.e., decide when to charge a vehicle). Such an approach allows a primary recasting of the decision-making problem as a classification task, where we want to identify the optimal action of a new observation. The principal learning methods proposed are Threshold-Based Rule, k-Nearest Neighbors, Shallow Neural Network, and Deep Neural Networks.

It should be noted that while we currently apply these methods offline — the training is conducted on a full dataset built from historical data — it would be easy to move torwards a fully online mode where the models would be trained incrementally or frequently, while providing predictions from the beginning.

3.4.1 Threshold-Based Rule

we propose to use a simple TBR over electricity price, where the threshold is computed over the current charge level with a sigmoid function

$$f(SoC, p_1, p_2) = \frac{1}{1 + \exp[-p_1(SoC - p_2)]},$$

with parameters p_1 and p_2 being optimized with the CMA-ES method [30], based on the objective function given in Eq. 3.

The decision rules on charging or standby mode with the TBR policy relies on the normalized electricity price $C_{el}(t)$ which takes values between 0 and 1 and SoC:

$$a(t) = \begin{cases} 1 \text{ (charge)} & \text{if } C_{el}(t) \leq f(SoC(t), p_1, p_2) \\ 0 \text{ (standby)} & \text{otherwise} \end{cases}. \tag{12}$$

3.4.2 k-Nearest Neighbors

here, each state is classified by a majority vote of its nearest neighbors (according to a distance metric, e.g. Euclidean) in the training dataset, with the state being assigned to the most frequent charge/standby action among its k nearest neighbors. In our setting, the training instances are formed as presented in Sec. 3.3, and the optimal decision (charge or standby) computed by DP. The optimal number of neighbors k to use is determined by cross-validation.

3.4.3 Shallow Neural Network

here we combine clustering, feature selection and a SNN with two layers, where the hidden layer is using a sigmoid transfer function and the output layer is linear, trained with the Levenberg-Marquardt algorithm. We first select a small representative sample of data using clustering, with the methodology of **(author?)** [29]. Then, we use a sequential stepwise process, called Backward Greedy Selection, to remove variables (features) that degrade — or do not sufficiently improve — neural network performance.

Table 3: Average gain (in %) for the 17 vehicles with respect to the basic 10-bins scheme for each Δ_t, in the summer and winter training periods.

	Δ_t	**Mean gain (standard dev.) by number of bins**			
	(min)	**20**	**30**	**50**	**100**
Summer	15	2.65 (0.23)	2.94 (0.27)	3.75 (0.28)	4.09 (0.25)
	30	5.34 (2.75)	5.95 (2.95)	6.38 (3.20)	7.85 (3.23)
	60	0.78 (1.01)	1.06 (0.94)	1.10 (0.95)	1.25 (0.94)
Winter	15	2.40 (0.28)	2.94 (0.31)	4.22 (0.26)	4.38 (0.29)
	30	6.26 (3.20)	6.62 (3.20)	6.85 (3.14)	8.25 (3.17)
	60	0.69 (0.60)	0.76 (0.62)	0.87 (0.61)	0.98 (0.62)

3.4.4 Deep Neural Networks

unlike SNN, DNN facilitates learning a hierarchical representation of the data, where each layer of neurons represents a level in that hierarchy. This property allows a representation to be learned from a large set of interrelated variables, which cannot be provided by separately trained variables. We propose to explore the use of a DNN to exploit the strong correlation present in our complex dataset formed with the data from all vehicles. Our DNN is fully connected with 508 inputs, four hidden layers (with 256, 96, 64 and 32 neurons, respectively) and one output layer of a single neuron interpreted as $a(t)$ in Eq. 1. Each layer uses Exponential Linear Unit (ELU) as an activation function, except the output layer which uses a softmax function. A batch normalization operation is added after each fully connected layers to encourage convergence. The network is trained with adaptive stochastic gradient descent (i.e., Adagrad [31]), which can adapt the effective (gradient) step size to improve and speed up convergence.

4 Results and Discussion

4.1 Dynamic Programming Model

First, we define the hyper-parameters of the decision model using DP. Table 3 presents the average gain of 17 vehicles over the basic $b = 10$ bins scheme using the DP model, in both seasons (summer and winter) on the training set, with a different time interval ($\Delta_t = \{15, 30, 60\}$) and different number of bins in the SoC discretization.

The results of Table 3 are products of the following equation:

$$\overline{\mathrm{G}}_{\Delta_t,\mathrm{Bin}=b} = \frac{1}{17}\sum_{i=1}^{17}\frac{\mathrm{C}_{i_{\Delta_t,\mathrm{Bin}=10}} - \mathrm{C}_{i_{\Delta_t,\mathrm{Bin}=b}}}{\mathrm{C}_{i_{\Delta_t,\mathrm{Bin}=10}}}, \tag{13}$$

where $\mathrm{C}_{i_{\Delta_t,\mathrm{Bin}=10}}$ represents the cost evaluated in the vehicle i for Δ_t when the SoC variable was discretized in 10 bins and $\mathrm{C}_{i_{\Delta_t,\mathrm{Bin}=b}}$ indicates the estimated cost in vehicle i for Δ_t when a different number of bins (b) was used. In this case $b \in \{20, 30, 50, 100\}$ state discretizations were tested.

In Table 3, we can identify a linear trend between the average gain and the increase in the number of bins used for discretizations, for both summer and winter periods. When looking at the coefficient of variation (standard deviation/mean), which describes the amount of variability relative to the mean, we can observe a very low spread of results for $\Delta_t = 15$ minutes with an average value of 8.3%, opposed to a spread of 47% for $\Delta_t = 30$ minutes and 85.2% for $\Delta_t = 60$ minutes.

Fig. 2 shows a direct relation between the length of the time interval and the operational charging cost (Eq. 4). Compared to a time interval of 15 minutes, using an interval of 60 minutes significantly hinders the effectiveness of

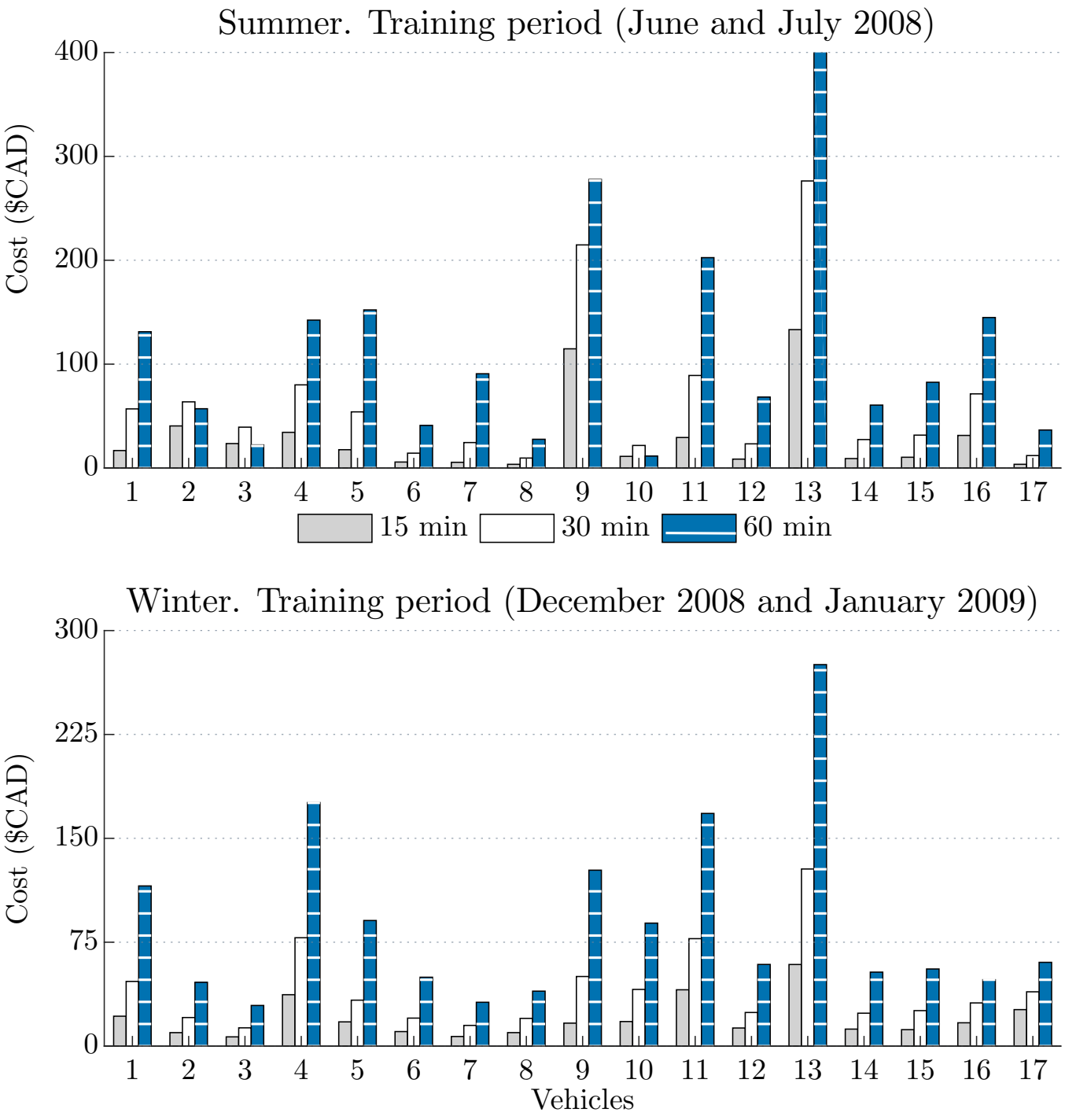

Figure 2: Average cost for the different number of bins by Δt for summer and winter training periods.

Table 4: Cost and gain regarding the gasoline price for the DP and AC models in summer and winter test datasets, for the 17 vehicles evaluated.

	Summer			**Winter**		
	Gas	DP	AC	Gas	DP	AC
	$	**$** (%)	**$** (%)	**$**	**$** (%)	**$** (%)
1	131.2	34.0 (74)	91.0 (31)	65.1	7.9 (88)	29.1 (55)
2	93.0	22.1 (76)	57.4 (38)	45.5	5.4 (88)	22.2 (51)
3	52.4	1.5 (97)	16.4 (69)	34.9	5.5 (84)	20.5 (41)
4	187.4	15.7 (92)	60.6 (68)	66.5	7.4 (89)	27.2 (59)
5	230.8	66.8 (71)	165.6 (28)	58.8	6.3 (89)	24.6 (58)
6	93.2	3.3 (96)	24.7 (73)	79.2	19.4 (76)	55.8 (29)
7	81.0	3.2 (96)	21.4 (74)	40.5	4.2 (90)	18.3 (55)
8	66.5	3.0 (95)	21.0 (68)	42.9	4.6 (89)	19.3 (55)
9	228.4	87.1 (62)	207.2 (9)	31.9	2.8 (91)	13.8 (57)
10	64.4	1.4 (98)	17.7 (73)	66.0	8.4 (87)	28.1 (57)
11	156.8	17.3 (89)	56.5 (64)	108.3	14.2 (87)	44.4 (59)
12	72.2	2.5 (97)	23.3 (68)	64.2	7.4 (88)	26.4 (59)
13	364.3	98.0 (73)	232.5 (36)	178.0	49.6 (72)	133.8 (25)
14	122.1	5.0 (96)	34.9 (71)	36.1	3.6 (90)	15.1 (58)
15	20.8	0.4 (98)	6.2 (70)	61.8	6.4 (90)	25.8 (58)
16	32.0	2.3 (93)	9.6 (70)	52.8	7.2 (86)	23.0 (56)
17	57.7	1.6 (97)	17.3 (70)	23.8	2.4 (90)	10.9 (54)
Mean gain		**88%**	**58%**		**87%**	**52%**
Median gain		**95%**	**68%**		**88%**	**56%**

DP. This is expected as a small time interval provides greater flexibility to the decision-making process. However, a finer time interval also implies a substantial increase of the model complexity.

The computation time for DP and the size of the datasets used with the ML methods are both increasing linearly with the number of bins used. From results presented above, $b = 20$ bins appears to be a satisfactory tradeoff, as the gains for increased number of bins are relatively modest, while it significantly increases the computational burden associated with the approaches evaluated. From this point onwards, the results presented are computed on the test datasets (not used to train/infer the models), with a SoC discretization of $b = 20$ equally spaced bins and a response interval of $\Delta t = 15$ minutes, (i.e. 96 time slots per day).

4.2 Always Charge Model

The AC model is a common strategy assuming the vehicle is charged as soon as it is parked, as long as its battery is not full. Table 4 shows the cost of each vehicle for three situations: 1) when it depends exclusively on gas, 2) using an optimal charging strategy (DP), and 3) using a simple AC strategy. We also calculate the savings according to the cost using gasoline (values in parentheses: $[\$\text{GAS} - \$\text{Model}]/\$\text{GAS}$).

We can observe in Table 4 that, in general, the AC model allows for significant savings in summer (28% to 74%), except for vehicle 9, which is amongst the vehicles with the greatest distance travelled, where the savings are only 9%. Also, the charge periods of this vehicle coincide with the peak energy prices. In this respect it can be observed that the savings of both AC and DP models are roughly inversely proportional to the distance travelled by the vehicle (i.e., vehicles 1, 5, 9, and 13 in the summer).

Table 4 shows the effect of these gain outliers in the difference between the mean and the median of the gain, a situation that is not reflected in the winter analysis, where the values are similar. However, it is worth highlighting

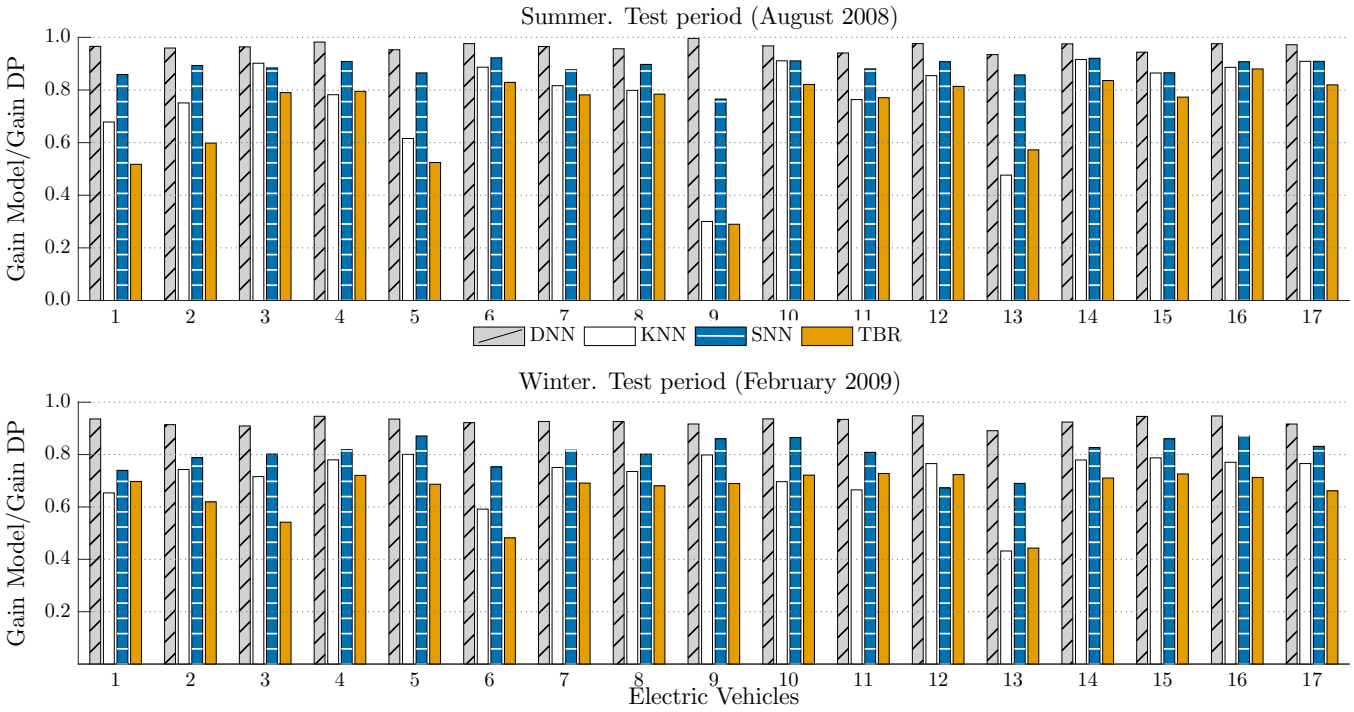

Figure 3: Relation of different ML models on the summer and winter test periods for 17 vehicles tested. For each method, the result is defined as the ratio between the cost reduction achieved by the method and the optimal cost reduction determined with DP. See Table 4 for the absolute gain values.

the efficiency of the simple AC strategy, which obtains median gains of 68% and 56% for summer and winter respectively. Indeed, the low electricity price on the market significantly decreases the overall energy cost of an EV, compared to a gasoline vehicle. This is true even for the AC worst case scenario, namely always charging when the electricity price is at its highest. Nonetheless, it is quite clear that the results can be further enhanced to close the gap with the optimal reference, which is able to reach 95% and 88% median gains in summer and winter, respectively.

4.3 Machine Learning Models

Fig. 3 shows the ratio between ML models and DP savings according to the cost of using gasoline. A value near 1 indicates a model with an efficiency close to the global optimum found with DP. As discussed in Sec. 2 and 3.4, this optimum value obtained with DP cannot be reached in real-life situations, since its computation requires perfect knowledge of the future. Accordingly, a gain below 1.0 does not indicate that a method is falling behind a better approach, but rather that without any information concerning the future, it was still able to recover a fraction of the performances obtained with optimal decisions provided by an oracle — most of it for methods such as SNN and DNN.

The DNN approach clearly stands out here, with a mean gain ratio of around 0.95, including a result as good as the global optimum for vehicle 9 in the summer session. Moreover, unlike DP which requires a perfect model of the future environment and is thus unsuitable for deployment, this DNN model can readily be applied in an operational, real-world context.

Other methods such as SNN are also strong performers, with average ratios of 0.88 and 0.80 in summer and winter sessions, respectively. This average is only 8% lower than the performance of DNN, which is of methodological importance. In particular, this shows that even a low-capacity model can be successfully applied given a careful

preselection of its input variables. For instance, a good subset of variables may help to establish driving habits and typical driving schedules, which is of importance when it comes to making a charge decision.

Finally, the KNN method presents average gain ratios of 0.77 and 0.72 and the TBR method presents average ratios of 0.71 and 0.66 in summer and winter respectively. Although these methods do not reach the DNN and SNN performances, they are still significantly better than a simple strategy such as AC.

5 Conclusions

In this paper, we proposed different models to determine when to charge an Electric Vehicle (EV) considering only the current state of the vehicle, without the need to make independent predictions on variables such as electricity price, demand, time of connection or amount of energy needed for a future trip.

Our models are based on two main principles: (i) that an optimal set of actions can be retrieved assuming a hypothetical case where we have a perfect knowledge of the future (i.e., to make an analysis on historical data to select the best moments to charge using Dynamic Programming (DP)); and (ii) these optimal actions, in combination with an information system, can be used to learn which variables and under what conditions the charging decisions should be made, using Machine Learning (ML) algorithms. Given these conditions, and provided that our battery model broadly matches the one in the vehicle, our approach can be readily applied to any kind of EVs.

Several alternatives were explored with various degrees of complexity, starting with a simple Always Charge (AC) model where vehicles always charge their batteries when plugged in, followed by a Threshold-Based Rule (TBR) model, in which the decisions are made using a dynamic threshold according to electricity price and battery State of Charge (SoC). Subsequently, we evaluate the performance of ML models: k-Nearest Neighbors (KNN), Shallow Neural Network (SNN), along with a Deep Neural Network (DNN) implementation.

Experimentally, we evaluate the DP performance by calculating the savings relative to the cost using gasoline ($[\$GAS - \$Model]/\$GAS$). These results revealed an average saving of 88% and 87% in summer and winter, respectively. Finally, we calculated the savings for each proposed ML technique and we normalized them according to the DP savings (a value of 1 thus indicates an optimal model).

The results were conclusive: the greater the complexity of the technique, the closer to the global optimum were the savings, with ratios close to 0.7 for the KNN and TBR techniques, and 0.88 and 0.80 in the summer and winter for the SNN model. The technique with the greatest impact was DNN with a mean ratio of 0.95. This therefore demonstrates how the combination of an offline optimization method (such as DP) and DNN can provide a solution very close to the global optimum, without loss of applicability in real-world conditions. As future work, it will be interesting to investigate the impact of a fleet of vehicles using this approach on the load curve, and using game theory to motivate different charging decisions.

Acknowledgements

We are grateful to Darwin Brochero for suggestions and critical review and Annette Schwerdtfeger for proofreading the paper. This work was supported by funding from FRQNT-Québec, Mitacs, E Machine Learning Inc., and NSERC-Canada. Computational resources have been provided by Calcul Québec / Compute Canada.

References

[1] J. Zazo, S. Zazo, and S. Valcarcel Macua. Robust worst-case analysis of demand-side management in smart grids. *IEEE Transactions on Smart Grid*, 8(2), 2017.

[2] Y. Mou, H. Xing, Z. Lin, and M. Fu. Decentralized optimal demand-side management for PHEV charging in a smart grid. *IEEE Transactions on Smart Grid*, 6(2), 2015.

[3] Z. Fan. A distributed demand response algorithm and its application to PHEV charging in smart grids. *IEEE Transactions on Smart Grid*, 3(3), 2012.

[4] P. Finn, C. Fitzpatrick, and D. Connolly. Demand side management of electric car charging: Benefits for consumer and grid. *Energy*, 42(1):358 – 363, 2012.

[5] S. Shao, M. Pipattanasomporn, and S. Rahman. Grid integration of electric vehicles and demand response with customer choice. *IEEE Transactions on Smart Grid*, 3(1), 2012.

[6] Q. Wang, X. Liu, J. Du, and F. Kong. Smart charging for electric vehicles: A survey from the algorithmic perspective. *IEEE Communications Surveys Tutorials*, 18(2), 2016.

[7] J. García-Villalobos, I. Zamora, J.I. San Martín, F.J. Asensio, and V. Aperribay. Plug-in electric vehicles in electric distribution networks: A review of smart charging approaches. *Renewable and Sustainable Energy Reviews*, 38, 2014.

[8] Changsun Ahn, Chiao-Ting Li, and Huei Peng. Optimal decentralized charging control algorithm for electrified vehicles connected to smart grid. *Journal of Power Sources*, 196(23), 2011.

[9] Z. Ma, D. S. Callaway, and I. A. Hiskens. Decentralized charging control of large populations of plug-in electric vehicles. *IEEE Transactions on Control Systems Technology*, 21(1), 2013.

[10] J.C. Mukherjee and A. Gupta. A mobility aware scheduler for low cost charging of electric vehicles in smart grid. In *International Communication Systems and Networks (COMSNETS)*, 2014.

[11] Zhihao Li, A. Khaligh, and N. Sabbaghi. Minimum charging-cost tracking based optimization algorithm with dynamic programming technique for plug-in hybrid electric vehicles. In *Vehicle Power and Propulsion Conference (VPPC)*, 2011.

[12] E. Sortomme, M.M. Hindi, S.D.J. MacPherson, and S.S. Venkata. Coordinated charging of plug-in hybrid electric vehicles to minimize distribution system losses. *IEEE Transactions on Smart Grid*, 2(1), 2011.

[13] Iñaki Grau Unda, Panagiotis Papadopoulos, Spyros Skarvelis-Kazakos, Liana M. Cipcigan, Nick Jenkins, and Eduardo Zabala. Management of electric vehicle battery charging in distribution networks with multi-agent systems. *Electric Power Systems Research*, 110, 2014.

[14] L. Gan, U. Topcu, and S. H. Low. Optimal decentralized protocol for electric vehicle charging. *IEEE Transactions on Power Systems*, 28(2), 2013.

[15] He Yifeng, B. Venkatesh, and G. Ling. Optimal scheduling for charging and discharging of electric vehicles. *IEEE Transactions on Smart Grid*, 3(3), 2012.

[16] M. C. Falvo, G. Graditi, and P. Siano. Electric vehicles integration in demand response programs. In *International Symposium on Power Electronics, Electrical Drives, Automation and Motion*, 2014.

[17] Alexander Schuller. Charging coordination paradigms of electric vehicles. In Sumedha Rajakaruna, Farhad Shahnia, and Arindam Ghosh, editors, *Plug In Electric Vehicles in Smart Grids: Charging Strategies*. Springer, 2015.

[18] L. Jia and L. Tong. Dynamic pricing and distributed energy management for demand response. *IEEE Transactions on Smart Grid*, 7(2), 2016.

[19] N. Rotering and M. Ilic. Optimal charge control of plug-in hybrid electric vehicles in deregulated electricity markets. *IEEE Transactions on Power Systems*, 26(3), 2011.

[20] S. Sarabi and L. Kefsi. Electric vehicle charging strategy based on a dynamic programming algorithm. In *International Conference on Intelligent Energy and Power Systems (IEPS)*, 2014.

[21] Yann LeCun, Yoshua Bengio, and Geoffrey Hinton. Deep learning. *Nature*, 521(7553), 2015.

[22] X. Qiu, L. Zhang, Y. Ren, P. N. Suganthan, and G. Amaratunga. Ensemble deep learning for regression and time series forecasting. In *IEEE Symposium on Computational Intelligence in Ensemble Learning (CIEL)*, 2014.

[23] Seunghyoung Ryu, Jaekoo Noh, and Hongseok Kim. Deep neural network based demand side short term load forecasting. In *IEEE International Conference on Smart Grid Communications (SmartGridComm)*, 2016.

[24] Elena Mocanu, Phuong H. Nguyen, Madeleine Gibescu, and Wil L. Kling. Deep learning for estimating building energy consumption. *Sustainable Energy, Grids and Networks*, 6, 2016.

[25] Zhiguang Wang, Weizhong Yan, and Tim Oates. Time series classification from scratch with deep neural networks: A strong baseline. *CoRR*, 1611.06455, 2016.

[26] A. Ashtari, E. Bibeau, S. Shahidinejad, and T. Molinski. PEV charging profile prediction and analysis based on vehicle usage data. *IEEE Transactions on Smart Grid*, 3(1), 2012.

[27] Richard Bellman. *Dynamic Programming*. Dover Publications, 1957.

[28] Hong-Guang Ma and Chong-Zhao Han. Selection of embedding dimension and delay time in phase space reconstruction. *Frontiers of Electrical and Electronic Engineering in China*, 1(1), 2006.

[29] Karol Lina Lopez, Christian Gagné, German Castellanos-Dominguez, and Mauricio Orozco-Alzate. Training subset selection in hourly Ontario energy price forecasting using time series clustering-based stratification. *Neurocomputing*, 156, 2015.

[30] Nikolaus Hansen. The CMA evolution strategy: a comparing review. In *Towards a new evolutionary computation*. Springer, 2006.

[31] John Duchi, Elad Hazan, and Yoram Singer. Adaptive subgradient methods for online learning and stochastic optimization. *Journal of Machine Learning Research*, 12, July 2011.

[32] Shuo Pang, J. Farrell, Jie Du, and M. Barth. Battery state-of-charge estimation. In *American Control Conference*, volume 2, 2001.

[33] O. Sundström and Binding C. Optimization methods to plan the charging of electric vehicle fleets. In *International Conference on Control, Communication and Power Engineering*, 2010.

[34] B. Xiao, Y. Shi, and L. He. A universal state-of-charge algorithm for batteries. In *Design Automation Conference*, 2010.

[35] Jung Seunghun and Kang Dalmo. Multi-dimensional modeling of large-scale lithium-ion batteries. *Journal of Power Sources*, 248, 2014.

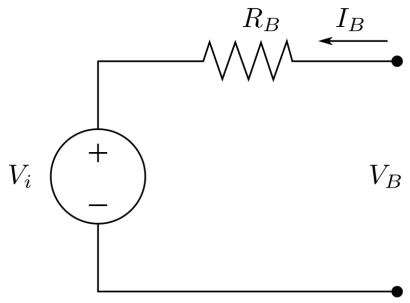

Figure 4: Battery Model.

A State of charge of Lithium-Ion battery

Since the battery is a nonlinear system, the modelling can be complex. We propose to use a simplified model with an equivalent electric circuit containing a voltage source in series with a resistor, which is described by Eq. 15 in order to estimate the State-of-Charge (SoC(t)). The model implements an ideal voltage source $V_{oc}[V]$ that represents the open-circuit voltage of the battery (voltage between the battery terminals with no load applied). The open circuit voltage V_{oc}, is known to be a function related to remaining SoC [32]. For the battery pack being considered herein, a full battery pack ($SoC = 100\%$) corresponds to a voltage of $N_s \cdot V_{max}$ volts. And, an empty battery pack ($SoC = 0\%$) corresponds to a voltage of $N_s \cdot V_{min}$ volts.

$R_B[\Omega] = \dfrac{N_s}{N_p} \cdot R_{cell}$ describes the internal resistance of the battery, N_s and N_p are the number of battery cells of the battery pack connected in serial and parallel form, respectively. $I_B[A]$ is the battery current. $V_B[V]$ is the battery terminal voltage. This model is very simple, but previous experiments indicate that the linear approximation is sufficient when considering the electric vehicle charging plan optimization [33]:

$$V_B(t) = V_{oc}(t) + R_B \cdot I_B(t), \tag{14}$$

$$V_{oc}(t) = SoC(t) \cdot V^* + N_s \cdot V_{min}, \tag{15}$$

where $V^* = N_s(V_{max} - V_{min})$, V_{min} is the minimum allowable cell voltage (Cut-off Voltage). V_{max} is the maximum cell voltage and I_B is the battery current.

The State of Charge $SoC(t)[\%]$ is the present battery capacity as a percentage of maximum capacity. $SoC(t)$ is not directly measurable, it is estimated based on the amount of charge that has been supplied or extracted from the battery and can be simply calculated as [34]:

$$SoC(t) = SoC(0) + \frac{1}{Q_{nom}} \int_0^t I_B(t)dt. \tag{16}$$

$Q_{nom}[Ah] = N_p \cdot Q_{cell}$ is the capacity of the battery pack, t_{dh} is the time of discharge at a constant current of discharge I_{dh}.

B Charging the battery pack

The batteries should be charged in two phases. During the first phase, the current is constant at I_{Bmax} and the voltage increases linearly from V_{min} to V_{max}. During the second phase, the voltage remains constant at V_{max} and the current decreases exponentially. It is possible to calculate the charging time of each of the phases. However, if the initial charge is high, the charging process passes directly to the second phase without passing through the first phase.

Accordingly to this model, Eq. 15 can then be rewritten as follows:

$$V_B(t) = SoC(0) \cdot V^* + \frac{V^*}{Q_{nom}} \int_0^t I_B(t)dt + N_s \cdot V_{min} + R_B \cdot I_B(t) \tag{17}$$

There may be a first phase if the following condition is respected:

$$V_{oc}(0) < N_s \cdot V_{max} - R_B \cdot I_{Bmax} \tag{18}$$

We solve Eq. 15 for $t = 0$, so the condition (18) can be restated as:

$$SoC(0) < 1 - \frac{R_B \cdot I_{Bmax}}{V^*} \tag{19}$$

If the condition described by Eq. 19 is true, the current is constant at I_{Bmax}. Replacing $I_B(t)$ by I_{Bmax} in Eq. 17 we obtain:

$$V_B(t) = SoC(0) \cdot V^* + \frac{V^*}{Q_{nom}} I_{Bmax} \cdot t + N_s \cdot V_{min} + R_B \cdot I_{Bmax} \tag{20}$$

The first phase is completed when the voltage reaches the maximum value $V_B = Ns \cdot V_{max}$.

Then, we simply solve Eq. 20 for $t = \tau_1$:

$$\tau_1 = \frac{Q_{nom}}{I_{Bmax}} \left[1 - SoC(0) - \frac{R_B \cdot I_{Bmax}}{V^*} \right], \tag{21}$$

where τ_1 is the time of charge of the first phase.

Finally, the battery is charged when the voltage reaches the upper threshold voltage $V_B = Ns \cdot V_{max}$ and when the intensity of current decays exponentially and stabilizes at I_{Bmin} at about 5% of $1C_r$ [35] [6].

The derivative of Eq. 17 with respect to t is:

$$R_B \cdot \frac{dI_B(t)}{dt} + \frac{V^*}{Q_{nom}} \cdot I_B(t) = 0. \tag{22}$$

The integral of 22 in the interval $[0, t]$ is:

$$\int_0^t \frac{1}{I_B(t)} \cdot dI_B(t) = -\frac{V^*}{R_B \cdot Q_{nom}} \int_0^t dt. \tag{23}$$

Equation 23 is then solved for $t = \tau_2$:

$$\tau_2 = -\frac{R_B \cdot Q_{nom}}{V^*} \cdot \ln\left(\frac{I_{Bmin}}{I_{Bi}}\right), \tag{24}$$

where τ_2 is the time of charge of the second phase.

The current I_{Bi} is calculated from Eq. 15 before the second phase of the charging process begins, as follows:

$$I_{Bi} = \frac{(1 - SoC(0)) \cdot V^*}{R_B}. \tag{25}$$

If the first phase precedes the second phase, the initial current should be the same at the end of the first phase $I_{Bi} = I_{Bmax}$.

In summary, the charging time ($t_{ch} = \tau_1 + \tau_2$) is defined as follows:

[6] C_r is a measure of the rate at which a battery is discharged relative to its maximum capacity. A $1C$ rate means that the discharge current will discharge the entire battery in 1 hour. For a battery with a capacity of 100 Ah, a $2C$ rate would be 200 A and a $C/2$ rate would be 50 A.

Algorithm 1 Time of charge t_{ch}, τ_1 and I_{Bi}

Require: Q_{nom}, V^*, I_{Bmax}, I_{Bmin}, R_B and $SoC(0)$
  if $SoC(0) < 1 - \left(\frac{R_B \cdot I_{Bmax}}{V^*}\right)$ **then**
    $I_{Bi} = I_{Bmax}$;
    $\tau_1 = \frac{Q_{nom}}{I_{Bmax}} \left[1 - SoC(0) - \frac{R_B \cdot I_{Bmax}}{V^*}\right]$;
  else
    $I_{Bi} = \frac{(1 - SoC(0)) \cdot V^*}{R_B}$
    $\tau_1 = 0$
  end if;
  $\tau_2 = -\frac{R_B \cdot Q_{nom}}{V^*} \cdot \ln\left(\frac{I_{Bmin}}{I_{Bi}}\right)$;
  $t_{ch} = \tau_1 + \tau_2$;

- If Eq. 18 is respected:

$$t_{ch} = \frac{Q_{nom}}{V^*} \left[\frac{1}{I_{Bmax}}((1 - SoC(0)) \cdot V^* - R_B \cdot I_{Bmax}) - R_B \cdot \ln\left(\frac{I_{Bmin}}{I_{Bmax}}\right)\right]; \tag{26}$$

- else:

$$t_{ch} = -\frac{R_B \cdot Q_{nom}}{V^*} \cdot \ln\left(\frac{R_B \cdot I_{Bmin}}{(1 - SoC) \cdot V^*}\right). \tag{27}$$

C State of Charge Estimation

When we want to estimate $SoC(t)$ and the electric driving range in kilometers as a function of $SoC(t)$, we first calculate the time of charge t_{ch} with Algorithm 1 and then, we calculate the $SoC(t)$ with Algorithm 2.

For the electric driving range we use Eq. 28:

$$R_e \text{ [km]} = \frac{m_e \cdot 0.0470 \cdot SoC(t) \cdot E_{nom}}{\eta_d}, \tag{28}$$

where m_e [MPG$_e$] are the miles per gallon gasoline equivalent of vehicle (1 MPG$_e$ ≈ 0.0470 [km/kWh]), $\eta \in [0, 1]$ is the discharging efficiency; and E_{nom} is the nominal energy.

Fig. 5 shows the charge characteristics calculated with our model of batteries assuming that the vehicle is a Plug-in Hybrid EV (PHEV) similar to a Chevrolet Volt 2013, with Panasonic Lithium-ion NRC18650 batteries, with specifications shown in Table 5. The I_{Bmax} current is dependent on both the battery characteristics and the power of the battery charger. In particular, this current should be limited in order to avoid exceeding 15 A at the wall (120V, household current) for level 1 charging stations and 80 A for level 2.

In the case of PHEV, the distance of the trip (D_{trip}) may be greater that the driving range when using only power from its electric battery (R_e), because the gas engine works as a backup when the batteries are depleted. Once the battery is fully depleted, the fuel consumed (E_{gas}) is:

$$E_{gas} \text{ [l]} = k_d \cdot (D_{trip} - R_e), \tag{29}$$

where $D_{trip} - R_e$ is the distance travelled using gasoline when $D_{trip} > R_e$ and $k_d = C_d/m$ is a constant [l/km] allowing distance to be converted into volume of gasoline. m [MPG] is the miles per gallon specification of the vehicle and $C_d = 0.621371 \cdot 3.785$ (1 km $= 0.621371$ miles and 1 gallon $= 3.785$ L).

Table 5: Specifications of battery packs, based on Chevrolet Volt 2013 and Panasonic NRC18650 Li-Ion batteries.

Chevrolet Volt 2013 specifications	
Nominal System Voltage V_{nom}	355.2 V
Rated Pack Capacity Q_{nom}	45 Ah
Rated Pack Energy E_v	16.5 kWh
Fuel economy (electricity) m_e	98 mpg_e (35 kWh/100 miles)
Fuel economy (gasoline) m	37 mpg
Panasonic NRC18650 specifications	
Nominal Capacity Q_{nom}	2.75 Ah
Nominal Cell Voltage V_{cell}	3.6 V
Max. Cell Charge Voltage V_{max}	4.2 V
Cut-off Discharge Voltage V_{min}	2.5 V
Maximum Charge Current I_{max}	0.825 A
Constant Current Discharge I_{dh}	0.55 A
Cut-off Charge Current I_{min}	0.05 A

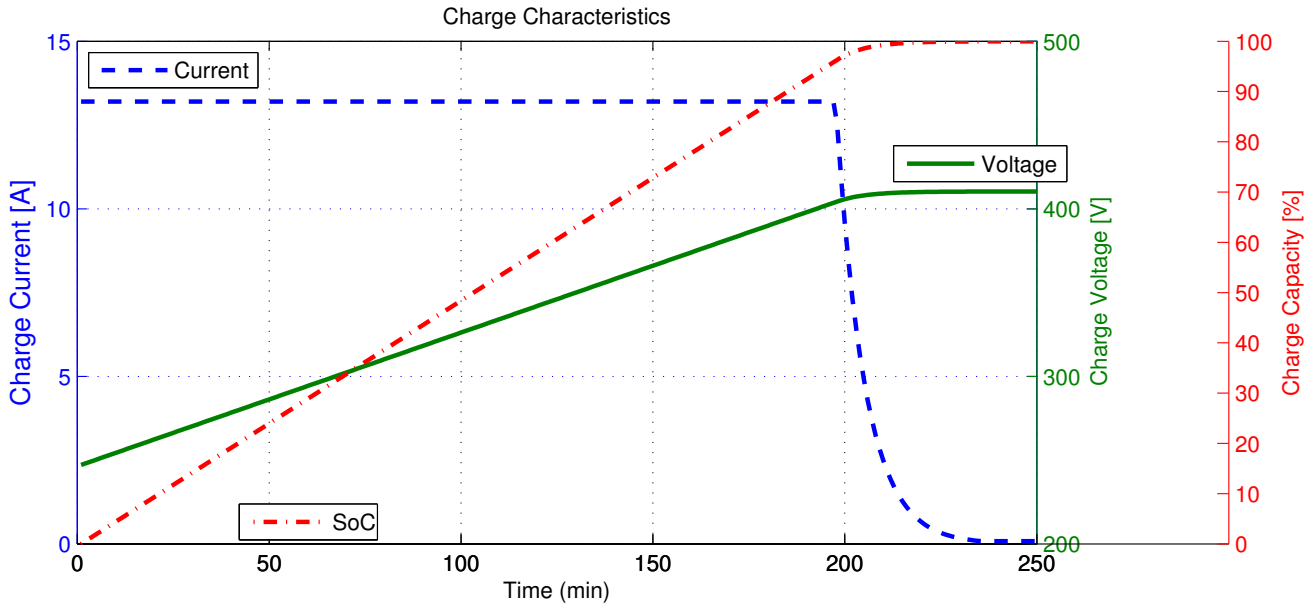

Figure 5: Charge characteristics calculated with the model of batteries used for the experiments.

Algorithm 2 State of charge $SoC(t)$ after charging during an interval of time Δ_t

Require: Q_{nom}, t_{ch}, τ_1, I_{Bi} and $SoC(0)$
  if $\tau_1 = 0$ **then**
    $$SoC(t) = SoC(0) + \frac{I_{Bi} \cdot min(t_{ch}, \Delta_t))}{Q_{nom}}$$
  else if $0 < \tau_1 < \Delta_t$ **then**
    $$w_1 = \frac{I_{Bi} \cdot \tau_1}{Q_{nom}}$$
    $$w_2 = \frac{I_{Bi} \cdot min(\Delta_t - \tau_1, t_{ch} - \tau_1))}{Q_{nom}}$$
    $$SoC(t) = SoC(0) + w_1 + w_2$$
  else if $\tau_1 >= \Delta_t$ **then**
    $$SoC(t) = SoC(0) + \frac{I_{Bi} \cdot \Delta_t}{Q_{nom}};$$
  end if;